LARGE STROKE ELECTROSTATIC COMB-DRIVE ACTUATORS BASED ON A NOVEL FLEXURE MECHANISM

Mohammad Olfatnia*[1], Siddharth Sood[1], Jason J. Gorman[2], Shorya Awtar[1]
[1]University of Michigan – Ann Arbor, USA
[2]National Institute of Standards and Technology, Gaithersburg, MD, USA

ABSTRACT

This paper presents in-plane electrostatic comb-drive actuators with stroke as large as 245 μm that is achieved by employing a novel Clamped Paired Double Parallelogram (C-DP-DP) flexure mechanism. For a given flexure beam length, comb gap, and actuation voltage, this is currently the largest comb-drive actuator stroke reported in the literature. The C-DP-DP flexure mechanism design offers high bearing direction stiffness while maintaining low motion direction stiffness over a large range of motion direction displacement. The high stiffness ratio between the bearing and motion directions mitigates the on-set of sideways snap-in instability, thereby offering significantly greater actuation stroke compared to existing designs.

INTRODUCTION

Electrostatic comb-drive actuators have been used in various applications such as resonators [1], and micro/nano positioning [2]. A linear in-plane electrostatic comb-drive actuator, shown in Fig. 1, comprises two electrically isolated conductive combs with N fingers each. While the static comb is fixed with respect to ground, the moving comb is guided by a flexure mechanism so that it can displace primarily in **Y** direction (or motion direction) with respect to the static comb. These static and moving comb fingers (length L_f, in-plane thickness T_f, out-of-plane thickness H_f) have a nominal inter-digitation gap of G and an initial engagement of Y_o. In general, the flexure mechanism is designed to provide linear displacement (Y) with relatively small stiffness (K_y) in the **Y** direction. Additionally, it provides minimal error motions (E_x) and relatively high stiffness (K_x) in the **X** direction, or bearing direction. In an ideal scenario, K_y and E_x would approach zero while K_x would approach infinity. However, in practice, this is never the case given the performance tradeoffs between motion range, stiffness, and error motions that exist in flexure mechanisms [3].
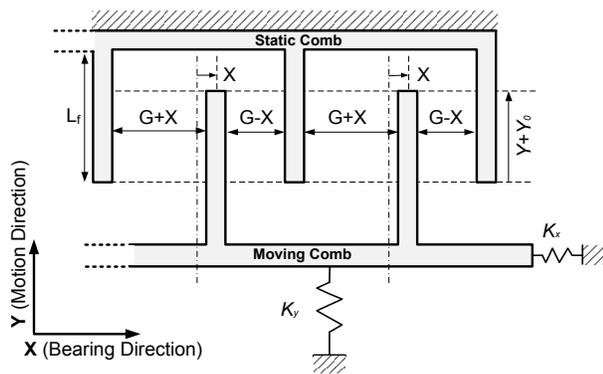

Fig. 1: Schematic of an electrostatic comb drive with the springs representing the flexure bearing.

When a voltage difference (V) is applied between the two combs, they experience a mutual electrostatic attraction, which displaces the moving comb by Y along the motion direction:

$$K_y \cdot Y = \frac{2\varepsilon N H_f G}{G^2 - X^2} V^2 \qquad (1)$$

Here, ε is the dielectric constant of air. The bearing direction displacement X can arise due to flexure error motion, fabrication misalignment, electrostatic forces, or disturbances in the **X** direction. While the displacement Y is determined by the comb geometry, motion direction flexure stiffness, and the actuation voltage, its maximum value (or actuation stroke) is limited by the snap-in phenomenon, which corresponds to side-ways instability of the moving comb [2, 4]. For any value of Y displacement, the electrostatic force due the actuation voltage V produces a destabilizing negative spring effect and the flexure mechanism offers a stabilizing positive spring effect in the **X** direction. The former increases with increasing stroke, while the latter generally decreases. The moving comb snaps sideways into the static comb at the Y displacement at which the former stiffness exceeds the latter. This condition may be mathematically expressed as [2, 5]:

$$\left(\frac{K_x}{K_y}\right) \leq \frac{2Y(Y+Y_0)}{G^2} \frac{\left(1+\frac{3X_c^2}{G^2}\right)}{\left(1-\frac{X_c^2}{G^2}\right)^2} \quad \text{where} \quad E_x = \frac{4X_c^3}{G^2 + 3X_c^2} \quad (2)$$

This snap-in condition assumes that the comb-fingers are perfectly rigid and all compliance comes from the flexure. Also, the in-plane rotation stiffness is assumed high enough to be ignored. The right hand side represents a "critical stiffness ratio" needed to avoid snap-in, and increases with displacement Y and error motion E_x. Clearly, to delay snap-in and maximize the actuator stroke, the flexure mechanism has to provide a high (K_x/K_y) ratio that is maintained over a large range of Y displacement. Since E_x is generally non-deterministic, the stability condition given by Eq.(2) may be mathematically simplified by incorporating a positive Margin of Stability (S). Stable operation is given by:

$$\left(\frac{K_x}{K_y}\right) \geq \frac{2Y(Y+Y_0)}{G^2}(1+S) \qquad (3)$$

The paired Double Parallelogram (DP-DP) flexure mechanism has been most commonly used in electrostatic comb-drive actuators [1, 2, 4]. While this flexure provides a high stiffness ratio (K_x/K_y) at $Y = 0$, K_x drops precipitously with increasing Y displacement even as K_y remains largely constant. This limits the comb-drive actuator stroke due to early snap-in. Pre-bent beams in the DP-DP flexure help shift the value of Y at which K_x is maximum, but do not restrict the drop in K_x with increasing Y [2]. This results in some improvement in the actuator stroke, but at the expense of robustness [5]. Other designs are successful at restricting the drop in K_x with increasing Y by appropriately constraining the secondary stage(s) in a DP or DP-DP flexure [6]. However, this also results in an increase in the motion direction stiffness, K_y, which is undesirable.

This paper presents a new Clamped Paired Double Parallelogram (C-DP-DP) flexure mechanism that offers high K_x over a large Y displacement range, while maintaining low K_y throughout. This new design is described in Section 2, along with closed-form analytical expressions for its K_x and K_y stiffness. With these improved stiffness characteristics, the C-DP-DP flexure is well suited for achieving large-stroke in comb-drive

actuators. Micro-fabrication of some representative actuators and associated experimental results are presented in Section 3. With the C-DP-DP flexure, a maximum actuation stroke of 245 µm with 1 mm flexure beam length and 6 µm comb finger gap is demonstrated.

FLEXURE MECHANISM DESIGN

In this section, we first discuss the traditional Paired Double Parallelogram (DP-DP), shown in Fig.2, which has been extensively studied previously [3, 4]. The advantages and limitations of this design provide the context for the proposed C-DP-DP flexure design that is discussed subsequently.

In all the designs considered here, we assume a general shape for each constituent beam, with two equal end-segments having uniform in-plane thickness T_1 and length a_0L_1 and a rigid middle section of length $(1-2a_0)L_1$. The geometric parameter a_0 quantifies the degree of distributed compliance; $a_0=1/2$ represents a uniform thickness beam with highly distributed compliance, while smaller values of a_0 correspond to increasingly lumped compliance. This parameter allows for subsequent beam shape optimization.
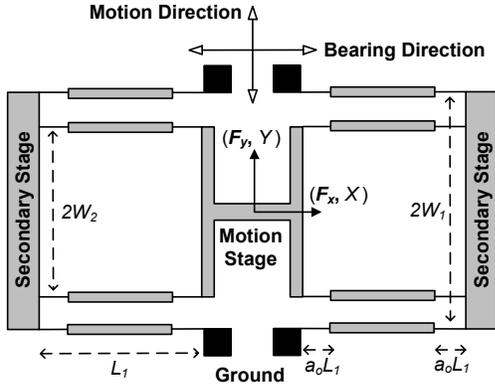

Fig. 2: Paired Double Parallelogram (DP-DP) flexure

Closed-form non-linear stiffness relations for this flexure geometry have been previously derived [3] and are summarized here:

$$K_y = \frac{2EI_1}{L_1^3}\left[k_{11}^{(0)} - \frac{1}{4k_{11}^{(0)}}\left(\frac{F_x L_1^2}{EI_1}k_{11}^{(1)}\right)^2\right] \quad (4)$$

$$K_x = \frac{2EI_1}{L_1^3}\frac{k_{33}}{\left(1 + k_{33}\left(k_{11}^{(2)} + \frac{\left(k_{11}^{(1)}\right)^2}{k_{11}^{(0)}}\right)\left(\frac{Y}{2L_1}\right)^2\right)} \quad (5)$$

Here, the non-dimensional terms $k_{11}^{(0)}$, $k_{11}^{(1)}$, $k_{11}^{(2)}$, and k_{33} are all functions of the beam shape (a_o and T_1) and are referred to as beam characteristic coefficients [3].

$$k_{11}^{(0)} = \frac{6}{\left(3 - 6a_o + 4a_o^2\right)a_o}$$

$$k_{11}^{(1)} = \frac{3\left(15 - 50a_o + 60a_o^2 - 24a_o^3\right)}{5\left(3 - 6a_o + 4a_o^2\right)^2}$$

$$k_{11}^{(2)} = \frac{2a_o^3\left(105 - 630a_o + 1440a_o^2 - 1480a_o^3 + 576a_o^4\right)}{175\left(3 - 6a_o + 4a_o^2\right)^3} \quad (6)$$

$$k_{33} = \frac{6}{a_0\left(T_1/L_1\right)^2}$$

As per Eq.(4), the DP-DP flexure provides a low K_y stiffness that remains constant with Y, and reduces to a simple expression in the absence of significant bearing force F_x. This motion direction stiffness depends directly on $k_{11}^{(0)}$. This mechanism also provides a high K_x stiffness at $Y = 0$, as per Eq.(5). However, this stiffness drops precipitously with increasing Y displacement (Fig. 3). Analytically, there are two sources of additional compliance, as seen in the denominator of Eq.(5). The first source arises from the elastokinematic effect manifested in the product $k_{33}k_{11}^{(2)}$, which approaches zero with reducing a_0. However, this is dominated by the second source that is based on the kinematic effect, manifested in the term $\left(k_{11}^{(1)}\right)^2 k_{33}/k_{11}^{(0)}$. The latter is at least two orders of magnitude greater than the former, is largely insensitive to variation in a_0, and never approaches zero. Therefore, as seen in Fig. 3, while the initial K_x / K_y ratio at $Y = 0$ can be increased by approaching lumped compliance (i.e. lower value of a_o), the impact of this shape variation is negligible at higher values of Y displacement.
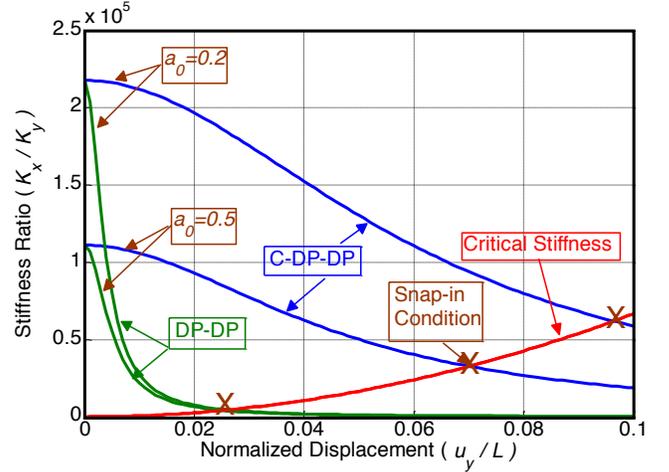

Fig. 3: (K_x/K_y) stiffness ratio provided by DP-DP and C-DP-DP flexures for different values of beam reinforcement (a_0). A typical critical stiffness curve is included to demonstrate the effect of stiffness ratio on comb-drive actuator snap-in.

This sharp decrease in the DP-DP flexure's K_x stiffness arises due to the mechanism's topology. In this design, the secondary stages of both the DPs are inadequately constrained in the Y direction. When the Y displacement of the motion stage is held fixed, and a small bearing direction force F_x is applied, the two secondary stages move opposite to each other in the motion direction from their nominal displacement of $Y/2$. This is because the motion direction stiffness of the each of the individual beams within the two DPs changes in the presence of F_x due to the load-stiffening effect. Due to this "extra" motion direction displacement of the two secondary stages, the kinematic error of the individual beams in the bearing direction no longer cancels out perfectly, thereby producing an "extra" X displacement at the motion stage and therefore a lower K_x.

Therefore, in order to avoid the above-described sharp decrease in the K_x stiffness, it is desirable to constrain the **Y** motion of both the secondary stages such that they always remain at their nominal value of $Y/2$, which is half the **Y** direction displacement of the motion stage. However, any topological feature that is considered to accomplish this should not restrict the small **X** direction displacements of each of these secondary stages. Restricting these displacements, which arise from the

kinematics of beam arc-length conservation, would lead to an over-constraint in the overall flexure mechanism, resulting in an increase in the motion direction stiffness, K_y.

We propose the Clamped Paired Double Parallelogram (C-DP-DP) flexure mechanism that accomplishes this goal via an external clamp, as shown in Fig. 4. In this design, the two secondary stages are connected to an external clamp through additional parallelogram flexures. The high rotational stiffness of these parallelogram flexures minimizes any relative displacement in the **Y** direction between the two secondary stages, forcing them to maintain $Y/2$ displacement at all times. This constrains these stages from responding to an **X** direction force on the motion stage. Also, the low **X** direction stiffness of the additional parallelogram flexures offers minimal resistance to the kinematic displacement of the secondary stages in the **X** direction.

The analytical relations for the motion and bearing stiffness of the C-DP-DP flexure have been separately derived [7] and are summarized here:

$$K_y = \frac{EI_1}{L_1^3}\left(2k_{11}^{(0)} + \frac{3k_{11}^{(0)}k_{11}^{(1)}}{20}\left(\frac{L_1^3}{L_3^3}\right)\left(\frac{Y}{L_1}\right)^2\right) \quad (7)$$

$$K_x = \frac{EI_1}{L_1^3}\frac{2k_{33}}{\left(1 + k_{33}\left(k_{11}^{(2)} + \frac{\left(k_{11}^{(1)}\right)^2}{k_{11}^{(0)}(1+\eta)}\right)\left(\frac{Y}{2L_1}\right)^2\right)} \; ; \; \eta = \left(\frac{6W_3^2 L_1^3}{k_{11}^{(0)}L_2^2 L_3 T_3^2}\right) \quad (8)$$

Motion Direction

Bearing Direction

L_3

$2W_3$

P   P

External Clamp

$2L_2$

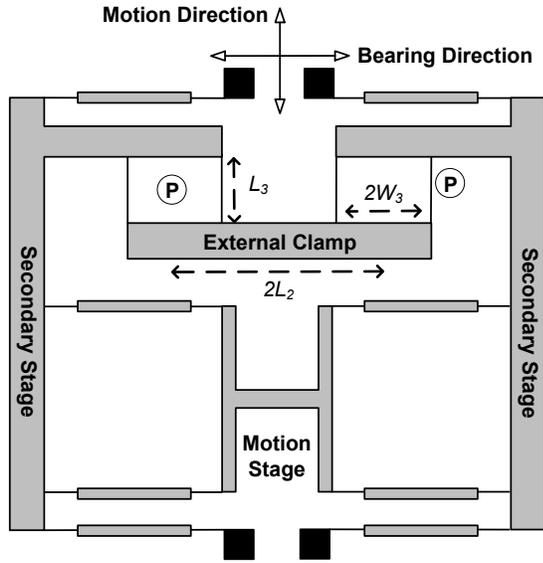**Secondary Stage** (left)   **Secondary Stage** (right)

Motion Stage

Fig. 4: Clamped Paired Double Parallelogram (C-DP-DP) flexure

Eq.(7) shows that there is a slight increase in K_y because of the external clamp. However, this can be mitigated by choosing a large enough beam length L_3 in the additional parallelograms. Next, the effectiveness of the clamp in restricting the precipitous drop in the bearing stiffness K_x is captured via the dimensionless parameter η in Eq.(8). The external clamp prevents relative **Y** direction motion between the two secondary stages by employing the high rotational stiffness of its constituent parallelograms, which manifests itself in the form of η. For low values of W_3, this stiffness and therefore η are small. It may be analytically seen that as $\eta \to 0$, the K_x stiffness becomes exactly the same as that for a DP-DP flexure, which corresponds to a completely ineffective clamp. However, as W_3 increases, the parameter η also increases. Eq.(8) shows that as η becomes very large, the kinematic term

$\left(k_{11}^{(1)}\right)^2 / k_{11}^{(0)}$ vanishes and only the elastokinematic term $k_{11}^{(2)}$ remains. Since the latter is at least two orders of magnitude smaller than the former, this implies that the drop in K_x stiffness now is significantly reduced and that the clamp proves to be effective. Furthermore, because of the sensitivity of the elastokinematic term to beam shape, reinforced beams ($a_0 < 0.5$) may be used to produce even greater improvements in the bearing stiffness K_x of the C-DP-DP flexure. This is in contrast with the DP-DP flexure for which beam reinforcement produces marginal benefits.

The (K_x / K_y) stiffness ratio for the C-DP-DP flexure for two different values of a_o is shown in Fig. 3, which demonstrates its superior stiffness characteristics compared to the DP-DP flexure. Also shown is a representative critical stiffness ratio curve for a typical comb-drive actuator, and the resulting snap-in conditions for the flexure designs considered here.

EXPERIMENTAL RESULTS AND DISCUUSION
Fabrication and Characterization

Several comb-drive actuators based on the DP-DP and C-DP-DP flexures were fabricated using silicon on insulator (SOI) wafers with a device layer of 50 µm, a buried oxide layer of 2 µm, and a silicon handle layer of 350 µm. First, the silicon handle layer was patterned and etched by deep reactive ion etching (DRIE); next, the buried oxide was removed by Hydrogen Fluoride (HF) etching; finally, the device layer was patterned and etched using DRIE. A scanning electron microscope (SEM) image of a representative comb-drive actuator is shown in Fig. 5. These actuators were driven using DC voltage applied via probes at the static and moving combs. The response of each actuator for a given voltage was observed with an optical microscope and video-captured with a CCD camera. Subsequently, the displacement of the actuator was extracted from the video using image processing software. The displacement measurements were repeatable within 1 µm.
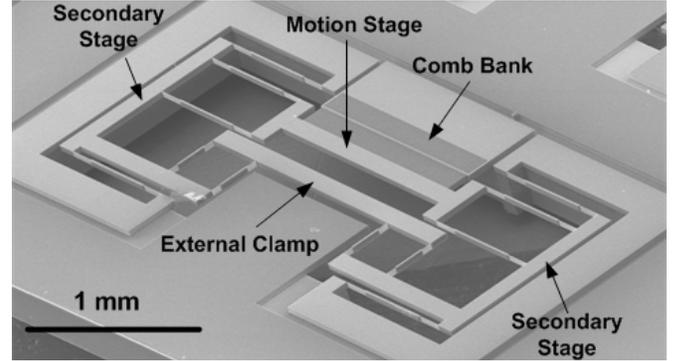

Fig. 5: SEM image of a fabricated C-DP-DP based comb-drive actuator.

Voltage-Stroke Curves

Fig. 6 shows the displacement versus voltage curves for comb-drive actuators based on three different flexures with $G = 3$ µm, $L_1 = 1$ mm, and $T_1 = 4$ µm. The measured actuator stroke with a conventional DP-DP flexure with these dimensions and $a_0 = 0.5$ was 50 µm. The actuation stroke increases to 119 µm for a C-DP-DP flexure with the same dimensions. This stroke further increases to 141 µm by using reinforced beams with $a_0 = 0.2$ in the C-DP-DP flexure. These results clearly highlight the effectiveness of the reinforced C-DP-DP in providing greater

comb-drive actuator stroke compared to the traditional DP-DP flexure.

By increasing the comb gap, the stroke of the comb-drive actuator can be further improved. This is demonstrated in Fig. 7, where a stroke of 215 μm was obtained by a C-DP-DP flexure with $G = 4$ μm, $L_1 = 1$ mm, and $a_0 = 0.2$. The benefit of beam reinforcement is also evident here. With an identical design, the experimentally measured stroke is 170 μm and 157 μm for $a_0=0.3$ and $a_0=0.4$, respectively. Finally, a large stroke of 245 μm at 120V for a C-DP-DP flexure with $G = 6$ μm, $L_1 = 1$ mm, and $a_0 = 0.2$ is also reported in this figure. For a given flexure beam length, comb gap, and actuation voltage, this is the largest comb-drive actuator stroke reported in the literature (Fig. 8), to the best of our knowledge. In general, it is desirable to minimize the product of the device footprint and operating voltage, while maximizing the stroke. This corresponds to the top-left corner of Fig. 8, which is where our present results lie.
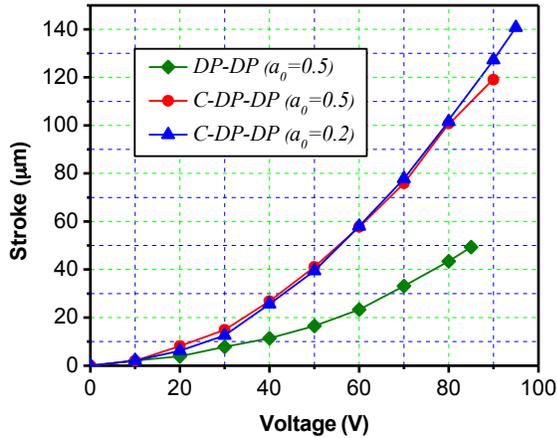

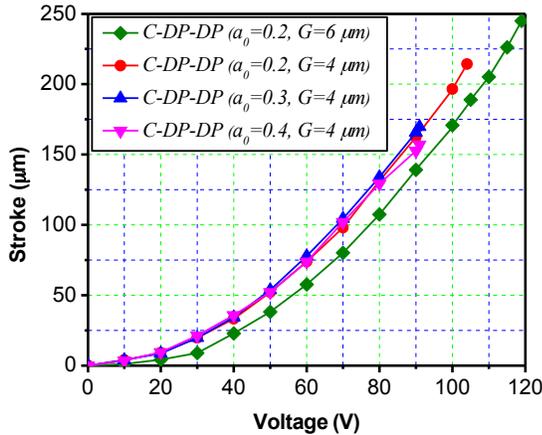Fig. 6: Displacement measurements for DP-DP and C-DP-DP flexures.

Fig. 7: Displacement measurements for C-DP-DP flexures.

CONCLUSION

This paper presents the Clamped Paired Double Parallelogram (C-DP-DP) flexure mechanism with reinforced beams, which offers high bearing direction stiffness (K_x) while maintaining low motion direction stiffness (K_y), over a large range of motion direction displacement (Y). It is shown that this flexure mechanism helps delay the on-set of snap-in instability in a comb-drive actuator and therefore provides greater actuation stroke. For 1 mm flexure beam length and 6 μm comb gap, strokes as large as 245 μm at 120 V have been demonstrated. This

experimental proof along with the analytical formulation clearly highlights the strength of C-DP-DP flexure for large range comb-drive actuators.
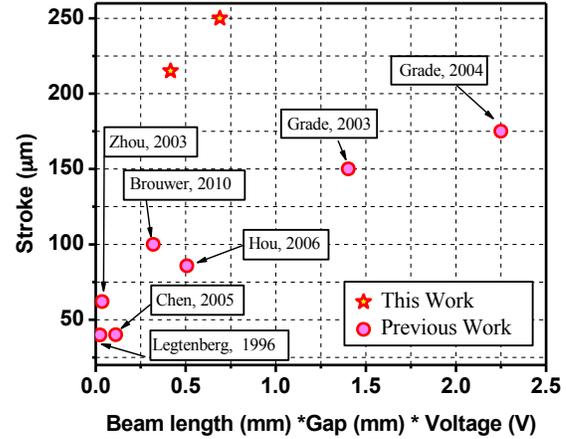
Fig. 8: Comparison of this paper's results with previously reported comb-drive actuator designs.

REFERENCES

[1] W. C. Tang, T. C. H. Nguyen, And R. T. Howe, "Laterally Driven Polysilicon Resonant Microstructures," *Sensors And Actuators,* Vol. 20, Pp. 25-32, 1989.

[2] J. D. Grade, H. Jerman, And T. W. Kenny, "Design Of Large Deflection Electrostatic Actuators," *Journal Of Microelectromechanical Systems,* Vol. 12, Pp. 335-343, 2003.

[3] S. Awtar, A. H. Slocum, And E. Sevincer, "Characteristics Of Beam-Based Flexure Modules," *Journal Of Mechanical Design,* Vol. 129, Pp. 625-639, Jun 2007.

[4] R. Legtenberg, A. W. Groeneveld, And M. Elwenspoek, "Comb-Drive Actuators For Large Displacements," *Journal Of Micromechanics And Microengineering,* Vol. 6, Pp. 320-329, 1996.

[5] S. Awtar And T. Trutna, "An Enhanced Stability Model For Electrostatic Comb-Drive Actuator Design," In *Proc. Idetc/Cie*, Montreal, Canada, 2010.

[6] D. M. Brouwer, A. Otten, J. B. C. Engelen, B. Krijnen, And H. M. J. R. Soemers, "Long-Range Elastic Guidance Mechanisms For Electrostatic Comb-Drive Actuators," In *Proceedings Of The Euspen International Conference*, Delft, 2010.

[7] S. Sood And S. Awtar, "Clamped Symmetric Double Parallelogram Flexure Mechanism With Improved Bearing Performance," In *Review Of Scientific Instruments*, Ed.

CONTACT

*M. Olfatnia, tel: +1-734-730-3141; olfatnia@umich.edu